applied optics

Signal-to-noise ratio enhancement of a Hadamard transform spectrometer using a two-dimensional slit-array

MINGBO CHI, YIHUI WU,* FANG QIAN, PENG HAO, WENCHAO ZHOU, AND YONGSHUN LIU

State Key Laboratory of Applied Optics, Changchun Institute of Optics, Fine Mechanics and Physics, Chinese Academy of Sciences, Changchun 130033, China

**Corresponding author: yihuiwu@ciomp.ac.cn*

Received 31 May 2017; revised 27 July 2017; accepted 6 August 2017; posted 7 August 2017 (Doc. ID 296711); published 29 August 2017

The encoding and decoding principle of the Hadamard transform spectrometer with a 2D slit-array mask is described in this paper. Based on the Hadamard transform theory, the signal-to-noise ratio (SNR) enhancement of a 2D slit-array Hadamard transform spectrometer is deduced and verified experimentally. Affected by the optical system of the spectrometer, there are differences between the experimental results and theoretical calculations. At the end of this paper, we discuss the influence of the spectrometer's optical system on the SNR enhancement based on the spatial frequency analysis.

OCIS codes: (120.6200) Spectrometers and spectroscopic instrumentation; (300.6190) Spectrometers.

https://doi.org/10.1364/AO.56.007188

1. INTRODUCTION

The traditional grating spectrometer uses a single slit to modulate the light signal from a diffuse source. The narrow slit, which can enhance the spectral resolution, will cause a loss of light and then decrease the signal-to-noise ratio (SNR) of the spectrometer [1]. In order to solve this contradiction between the SNR and the spectral resolution, Hadamard transform was introduced into the spectroscopy for the detection of weak diffuse sources [2–4]. This kind of spectrometer, called the Hadamard transform spectrometer, implements compound measurements of the spectral signals from different spectral channels to get an enhanced SNR while realizing a proper spectral resolution. However, this kind of spectrometer is not widely used for the lack of a high-precision encoding element, which is cheap and easily integrated. With the development of imaging detectors and high-precision manufacturing technology, a new kind of Hadamard transform spectrometer, which just uses an encoding mask with a 2D slit-array curved on it to replace the single slit of the traditional spectrometer, has been reported [5–7]. The 2D slit-array encoding mask shows great potential in the practicality of a Hadamard transform spectrometer due to its easy integration, small bulk, and low cost.

The SNR enhancement compared with the traditional single-slit spectrometer is the main performance index of the Hadamard transform spectrometer. Previous research mainly focused on the SNR enhancement from the Hadamard transform [2–4,8]. The computation of the SNR enhancement is usually based on the Hadamard transform theory, and the influence of the optical system is ignored. However, the practical SNR enhancement of the Hadamard transform spectrometer depends on the way it implements the encoding process. For the 2D slit-array spectrometer, the encoding mask and the optical dispersion system function together to implement the Hadamard transform, and its SNR enhancement comes both from the Hadamard transform and the multichannel simultaneous detection. In this paper, we make both theoretical and experimental analyses on the relationship between the SNR enhancement and the structure of the 2D slit-array. Based on experimental results and simulations in the spatial frequency domain, we discuss the influence of the optical system on the SNR enhancement of the spectrometer at the end of this paper.

2. THEORETICAL ANALYSIS FOR THE SNR ENHANCEMENT

As shown in Fig. 1, the 2D slit-array Hadamard transform spectrometer is mainly constructed of the 2D encoding mask, the optical system, and the imaging detector. The encoding process is mainly implemented by the encoding mask. The subslits in the same column belong to the same spectral channel as they generate the same spectral distribution on the detector plane because of the same location along the dispersion direction of the spectrometer. The spectral signals generated by the apertures in the same row multiple on the same pixel of the detector, which can be seen as a compound measurement of these spectral channels. In the binary encoding matrix, the code "1"

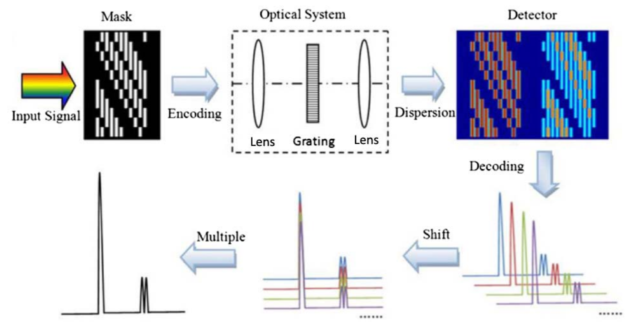

Fig. 1. Encoding and decoding principle of the 2D slit-array Hadamard transform spectrometer.

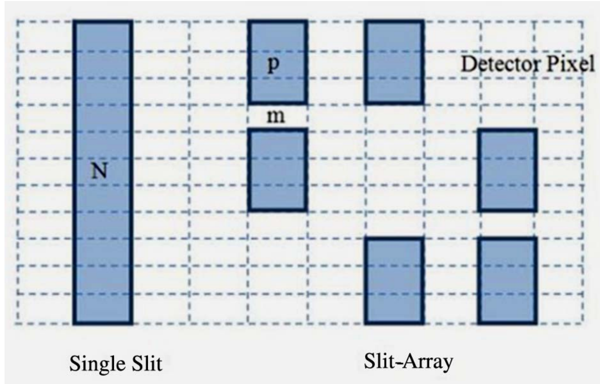

Fig. 2. Structure of the single slit and the 2D slit-array.

means that the spectral channel is included in the corresponding compound measurement and code "0" means it is not. The sets of spectral channels can be represented by a vector, ψ, the encoding matrix can be denoted by S, and the results of the compound measurements are denoted by η. Thus, the encoding equation can be described as follows:

$$\eta = S\psi. \tag{1}$$

If we use S^- to denote the inverse of S, the decoding equation is shown as follows:

$$\psi = S^-\eta. \tag{2}$$

Then we can get the decoded spectral distribution of each spectral channel whose SNR is enhanced by the decoding process or the inverse Hadamard transform process. As we can see, there is a wavelength shift between every two spectra channels, which is caused by the distance between the two columns of the apertures in the diffusion direction. After the calibration of the wavelength shift, all of the decoded spectra can be multiplied to get another SNR enhancement. Therefore, the total SNR enhancement of the spectrometer comes both from the Hadamard transform and the multichannel simultaneous detection.

It is well known that the SNR enhancement from the Hadamard transform is proportional to the order of the encoding matrix [2]. However, in the practical structure of the spectrometer, the encoding area of the slit-array is restricted by the area of the imaging detector. To make full use of the detector pixels, the height of the subslit in the array is designed to be integral multiplies of the detector pixel's height, as shown in Fig. 2. For a given detector, the maximum order of the 2D slit-array should be the number of rows of the detector pixels. The larger the order of the encoding matrix, the less pixels one subslit takes. Therefore, the spectrometer will be more sensitive to the decoded error caused by the misalignments of the subslit and the corresponding detector pixels as the increase of the order of the encoding matrix.

As shown in Fig. 2, the subslit in the slit-array corresponds to p rows of detector pixels and there are completely opaque rows of m rows of detector pixels placed between every two subslits to reduce the cross talk caused by the PSF of the optical system while the traditional single slit occupies N rows of pixels. If the order of the encoding matrix is denoted as n, then we can get

$$N = np + (n - 1)m. \tag{3}$$

When detecting weak signals, the noise can be seen as signal-independent pure additive detector noise. Provided that all pixels perform almost identically, the SNR of the single slit resulting from averaging N rows of pixels will be $N^{1/2}$ times the SNR achieved for a single pixel. Using a single pixel as a reference, the SNR enhancement of the single slit Q_s is

$$Q_s = \sqrt{N}. \tag{4}$$

When using a 2D slit-array, the SNR enhancement comes both from the Hadamard transform and the multichannel detection. Before the decoding process, we take the average of the signal in the p rows of pixels that correspond to the same subslit as the result of one compound measurement. Then we also use a single pixel as a reference. Each compound measurement can achieve an SNR gain Q_p through this averaging in the following equation according to Eq. (3):

$$Q_p = \sqrt{\frac{N - (n - 1)m}{n}}. \tag{5}$$

The SNR enhancement by the Hadamard transform depends on the order of the encoding matrix and the pattern of the encoding matrix. Usually, we chose a Hadamard S matrix as the encoding matrix, which is the best practical encoding matrix in experience [2]. Thus, after the decoding process, the SNR enhancement of each channel's decoded spectrum compared with the compound measurement is shown as

$$Q_H = \frac{n + 1}{2\sqrt{n}}. \tag{6}$$

Because of the wavelength shift caused by the column distance in the slit-array, the spectra of these channels at the same wavelength are generated from pixels in different columns of the detector. Thus, the decoded spectra are independent from each other. The SNR enhancement Q_n resulting from the averaging of the n channels of decoded spectra is shown as follows:

$$Q_n = \sqrt{n}. \tag{7}$$

Therefore, the total SNR enhancement of the 2D slit-array compared with a single pixel in the detector can be represented as follows:

$$Q_{\text{array}} = Q_p Q_H Q_n = \frac{n+1}{2}\sqrt{\frac{N-(n-1)m}{n}}. \quad (8)$$

Comparing Eq. (4) with Eq. (8), we can get the SNR enhancement by using a 2D slit-array to replace the single slit. The enhancement is given by

$$\frac{Q_{\text{array}}}{Q_S} = \frac{n+1}{2\sqrt{n}}\sqrt{\frac{N-(n-1)m}{N}}. \quad (9)$$

When the algorithm proposed in Ref. [9] is used to calibrate the decoded error caused by the cross talk between the adjacent compound measurements, the design of opaque rows can be removed. Then according to the Eq. (9), if the size of the imaging detector is given, then the smaller the number of rows of pixels corresponding to one subslit, the larger the order of the encoding matrix, and the larger the SNR enhancement compared with the traditional single slit. To increase the SNR enhancement, the coded apertures should be designed with high order and small subslit height. On the other hand, the small subaperture height makes the decoded spectrum sensitive to the system decoded error caused by manufacturing errors and the misalignment of the subslit and the detector pixels, which is a new trade-off needed to be balanced.

3. EXPERIMENT RESULTS AND SIMULATION ANALYSIS

Figure 3 illustrates the experimental setup used to test the SNR enhancement of the 2D slit-array spectrometer. The optical system of the spectrometer is the same as a traditional single-slit spectrometer. In all the experiments, a Hg lamp is chosen as the spectral source for its sharp spectral features. Modulated by the 2D slit-array, the incident light from the Hg lamp is collimated by a collimating mirror. The collimated light is subsequently dispersed by a grating and imaged on an imaging detector by a condensing mirror. The CCD detector translates the encoded light signal into a digital signal and transmits it to the computer for the decoding process.

We have manufactured four kinds of mask with different orders (3, 7, 15, and 31) through laser phototypesetting technology. For each kind of mask, two patterns of a 2D slit-array encoded, respectively, in the Hadamard S matrix and cyclic S matrix with the same order are curved on it to make a group of contrast experiments, as shown in Fig. 3. All the slit-arrays correspond to nearly the same encoding area of about 60 rows of pixels on the detector. The mask is mounted on a lifting stage, and the two patterns can be switched just through adjusting the height of the lifting stage in each group of contrast experiment while the other experimental setups remain the same. We have made five groups of contrast experiments using each kind of mask and detected the spectrum of the Hg lamp at 546 nm for 30 times in each group of experiments. All the measurements are made using the same light source, optical system, detector, and integration time. The raw encoded data in each group of contrast experiment is shown in Fig. 4.

Having implemented the same signal process algorithms, such as the smear noise removal algorithm and decoding algorithm on all the decoded data [9,10], we can get the decoded spectra of the Hg lamp. The SNR of the decoded spectrum is defined as the ratio of the mean and standard deviation of the decoded spectral intensity. In the Hg lamp spectrum, the spectral intensity changes rapidly with wavelength in the spectral region that only contains a sharp peak, and the spectra of different encoding channels have a wavelength shift between each other, as shown in Fig. 1. Then the intensity of one subslit's image in the encoded data shown in Fig. 4 can be seen as the measurement of the peak of the Hg lamp at 546 nm just using one single slit and a single pixel. In each group of experiments, we use the ratio of the SNR of the decoded intensities and the SNR of the peak intensities of one pixel in the encoded data as the normalized SNR enhancement when using a single pixel as the reference. This normalized method can remove the system error caused by light source fluctuation during the whole experiment process. According to Eq. (8), the theoretical SNR enhancement of these slit-arrays are calculated out and shown in Fig. 5(a) as well as the experimental SNR enhancement using the slit-array encoded in Hadamard S matrix and cyclic S matrix, respectively.

As we can see from Fig. 5(a), the experimental results are both in good agreement with the derived theoretical results when using the Hadamard matrix and the cyclic S matrix. The SNR enhancement increases as the slit-array order increases both in the theoretical calculation and the experimental results when the encoding area on the detector is given, though there are still differences between the experimental results and the theoretical calculations. In our opinion, the decrease of the

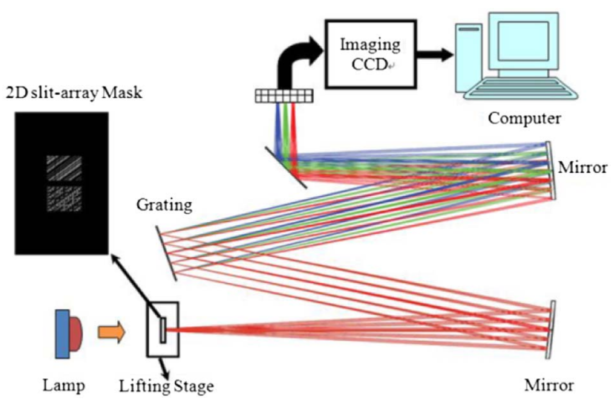

Fig. 3. Schematic of the experimental setup used to measure the SNR enhancement.

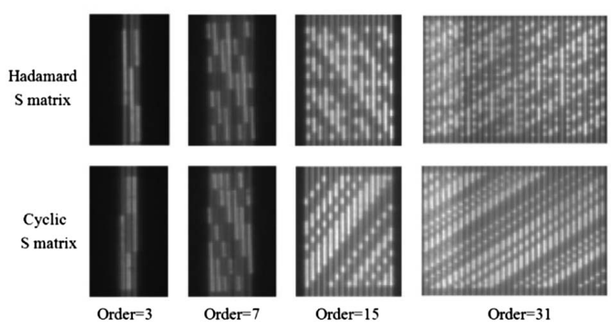

Fig. 4. Contrast of the encoded data of the slit-array with different orders and patterns on the detector.

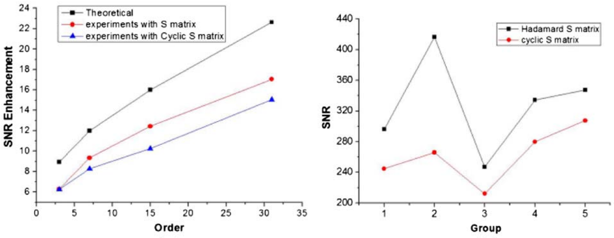

(a) (b)

Fig. 5. (a) SNR enhancement of the theoretical calculation and the experimental results using the Hadamard S matrix and the cyclic S matrix, respectively. (b) Mean of the SNR of the five groups of contrast experiments using the slit-array encoded in the Hadamard S matrix and the cyclic S matrix of order 31, respectively.

SNR gain in the experiments mainly arises from the optical system of the spectrometer, which implements the compound measurement of the encoded data. The compound measurement process can be seen as the imaging process of the 2D slit-array when detecting a monochromatic light. However, no optical system can realize the perfect imaging and there are always encoding errors in the compound measurements. The better the imaging quality of the optical system, the more accurately the compound measurement is implemented and the larger the SNR enhancement of the spectrometer. Besides, the errors in the experiment setup, for example, the misalignment of the mask and detector and the nonuniform illumination, will also cause a decrease in the SNR enhancement. Therefore, the practical SNR enhancement of the 2D slit-array is always lower than that in theory.

On the other hand, it can be derived from Eq. (9) that the SNR gain of the spectrometer mainly comes from the Hadamard transform, which only depends on the order and pattern of the encoding matrix when using a 2D slit-array without opaque rows, and the SNR gain of the slit-array using a cyclic S matrix should be identical to that of the Hadamard S matrix. However, with the same experiment setup and parameters of the subslit, the SNR gain of the slit-array encoded in the cyclic S matrix of each order is lower than that of the Hadamard S matrix, as shown in Fig. 5(a). Figure 5(b) shows the mean of the experimental SNR in each group of the five contrast experiments when using the two different slit-arrays of order 31, and the SNR of the cyclic S matrix is always lower than that of the Hadamard S matrix, too. This contradiction implies that the SNR gain of the slit-array is not only determined by the Hadamard transform and different patterns of the slit-arrays can also affect the SNR gain of the system in other ways.

The decoded spectral intensity should be proportional to the throughput of the spectrometer, which is mainly decided by the slit-array. Different patterns of the slit-array have different spatial frequency characteristics though they have the same number of slits. The optical system of the spectrometer is a linear shift-invariant system, which functions as a low-pass filter in the spatial frequency domain, and it gives different responses to different spatial frequencies. Therefore, the affect of the optical system on different slit-arrays is quite different, which will lead to the difference in the SNR enhancement.

In the specification of the slit-arrays and their transmission through the optical system to form an image on the detector, the spatial distribution of the input energy and its Fourier transform, the spatial frequency spectrum, are equivalent as long as linearity constraints are obeyed [11]. Thus, we can use the power spectrum of the image of the slit-array in the spatial frequency domain to estimate the throughput of the spectrometer with different patterns of the slit-array. The optical transfer function (OTF) is the transfer characteristic of the optical system in the spatial frequency domain and describes the attenuation of spatial frequency as it passes through the system. The spatial frequency representation of the slit-array's image can be found through the product of the spatial frequency spectrum of the slit-array in the object space and the OTF of the optical system. The spatial frequency power spectrum, in which phase has been discarded, can be seen as the square of the amplitude of the spatial distribution of the slit-array's image. Then we can use the integration of the spatial frequency power spectrum in the image space upon the interval below the cutoff frequency as the estimate of the throughput, which is denoted as T according to the Plancherel's theorem as follows:

$$T = \iint_{-f_c < f_x, f_y < f_c} |I(f_x, f_y)\mathrm{OTF}(f_x, f_y)|^2 \mathrm{d}f_x \mathrm{d}f_y. \quad \textbf{(10)}$$

Here (f_x, f_y) is the corresponding two-dimensional spatial frequency coordinate, $I(f_x, f_y)$ denotes the 2D spatial frequency spectrum in the object space, which is the Fourier transform of the spatial distribution of the slit-array, and $\mathrm{OTF}(f_x, f_y)$ denotes the optical transfer function of the optical system in the spatial frequency domain. The cutoff frequency of the optical system is denoted as f_c. Since the optical system can be seen as a low-pass filter, the more the spatial frequency spectrum of the slit-array concentrates on the low spatial frequency interval, the larger the throughput and the SNR enhancement of the spectrometer.

According to the analysis above, we have made a series of simulation computations for the distribution of amplitude of the 2D spatial frequency spectrum of the slit-array encoded in a Hadamard S matrix and a cyclic S matrix with different orders (3, 7, 15, and 31) by use of a Fourier transform. The simulation results of the slit-arrays with order 15 are shown in Fig. 6.

As we can see from the simulation results shown in Fig. 6, the amplitude representations of these two slit-arrays in the spatial frequency domain are quite different. The 2D slit-array encoded in a cyclic S matrix has obvious periodicity in the diagonal direction. Thus, its spatial frequency distribution concentrates on some high-frequency range. On the contrary, there is almost no periodicity in the distribution of the slit-array encoded in the Hadamard S matrix. Its spatial frequency distribution contains more low-frequency components and more energy can transform through the optical system, which is a low-pass filter in the space frequency domain. Based on the simulation calculations and Eq. (10), an estimate of the throughput of the spectrometer with different kinds of slit-arrays is made to qualitatively analyze the influence of the different spatial frequency spectra of the slit-array on the SNR of the spectrometer. The OTF of the spectrometer can be

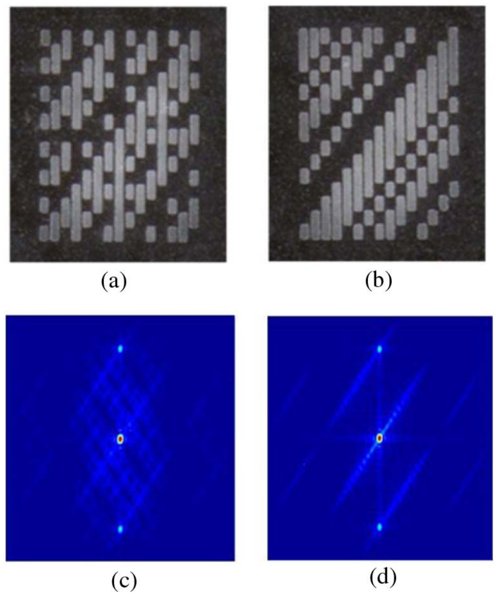

Fig. 6. (a) Image of the slit-array encoded in the Hadamard S matrix with order 15 under microscope. (b) Image of the slit-array encoded in the cyclic S matrix with order 15. (c) Simulation for the amplitude representation of the slit-array shown in (a) in the spatial frequency domain. (d) Simulation for the amplitude representation of the slit-array shown in (b) in the spatial frequency domain.

calculated based on the structure of the optical system of the spectrometer with the help of Zemax software. The calculation results for the throughput of the spectrometer using the slit-array encoded in Hadamard S matrix and cyclic S matrix of different orders (3, 7, 15, and 31) are shown in Fig. 7(a).

As shown in Fig. 7(a), the throughputs of the spectrometer using the slit-array encoded in both the Hadamard S matrix and the cyclic S matrix increase with the order of the encoding matrix and the throughput of the Hadamard S matrix is larger than that of the cyclic S matrix, which is consistent with the experimental results of the SNR enhancement shown in Fig. 5(a). By contrast, from the simulation results and the experimental results, it can be derived that the difference in the throughput of the spectrometer, which is caused by the different patterns of the Hadamard S matrix and the cyclic S matrix, will cause a difference in the SNR enhancement of the spectrometer.

Then we calculated the ratio of the simulation throughput and the ratio of the experimental SNR enhancement between the spectrometer using the Hadamard S matrix and the cyclic S matrix, as shown in Fig. 7(b). The ratio of the simulation throughput between the Hadamard S matrix and the cyclic S matrix is essentially identical to that of the experimental SNR enhancement when the order of the encoding matrix is less than 15. As the order increases, the ratio of the throughput and the SNR enhancement between the Hadamard S matrix and the cyclic S matrix increases. That implies that the larger the order of the encoding matrix, the larger effect the optical system of the spectrometer has on the SNR enhancement of the spectrometer. When using the slit-array with order 31, there is significant difference between the simulation result and the experimental result, which is mainly caused by the misalignment of the slit-array and the detector in our opinion. The subslit in the slit-array with order 31 in this paper only corresponds to two rows of detector pixels, and the largest misalignment is nearly 0.5 pixel, which is a quarter of the height of the subslit. Then the decoded spectrum is very sensitive to the decoded error caused by the misalignment, and a significant reduction in the SNR will occur in the slit-array both encoded in the Hadamard S matrix and the cyclic S matrix. However, the SNR enhancement of the Hadamard S matrix is still larger than that of the cyclic S matrix according to the experiment result shown in Fig. 7(b). Thus, the estimate of the throughput of the spectrometer based on the simulation in the spatial frequency domain can be used to compare the SNR enhancement of the slit-array encoded in different patterns of a matrix qualitatively.

4. DISCUSSION

The 2D slit-array Hadamard transform spectrometer's SNR enhancement increases as the increase of the order of the encoding matrix when the encoding area on the detector is given. In addition, the practical SNR enhancement of the spectrometer is also affected by the optical system and related to the spatial frequency distribution of the slit-array, which is mainly determined by the pattern of the encoding matrix. For two encoding matrices that have the same theoretical SNR enhancement based on the Hadamard transform theory, the more the amplitude representation of the slit-array in the spatial frequency domain concentrates on the low-frequency interval, the larger the throughput of the spectrometer, which is proportional to the SNR of the spectrometer. The estimate of the throughput of the spectrometer based on the simulation of the spatial frequency distribution of the slit-array can be used as a qualitative criterion for the choice and optimization of the encoding matrix to maximize the SNR enhancement of the spectrometer in the design of the slit-array in the future.

However, there are also some additional factors that need to be considered in the choice of the encoding matrix. Though the decoded error caused by the nonuniform illumination can be calibrated using the method that we proposed [9], the throughput and SNR of the system may be affected by the nonuniform illumination. Hadamard coding is a linear unbiased spectral

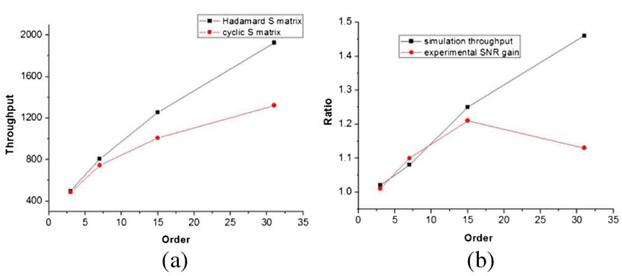

Fig. 7. (a) The simulation result for the throughput of the spectrometer using the slit-array encoded in the Hadamard S matrix and the cyclic S matrix of different orders. (b) The ratio of the simulation throughput and the ratio of the experimental SNR enhancement between the spectrometer using the Hadamard S matrix and cyclic S matrix.

estimator and the encoding matrix needs to be a nonsingular matrix. Unfortunately, the throughput advantage of multiplex measurements does not translate to an SNR advantage for a linear unbiased estimator when photon noise is dominant in the spectral signal [2]. Biased estimators using the regularization technique and iterative estimation algorithms are introduced to improve the estimation SNR, but these algorithms significantly impact the performance of different codes [12,13]. Further consideration of the influence of these factors on the choice and optimization of the encoding matrix will be made in future studies.

Funding. National Natural Science Foundation of China (NSFC) (61605198, 51505456); National High Technology Research and Development Program of China (2015AA042402).

REFERENCES

1. R. Riesenberg, A. Wuting, G. Nitzsche, and B. Harnisch, "Optical MEMS for high-end micro-spectrometers," Proc. SPIE **4928**, 6–14 (2002).
2. M. Harwit and N. Sloane, *Hadamard Transform Optics* (Academic, 1979), pp. 200–228.
3. R. A. Deverse, R. M. Hammaker, and W. G. Fateley, "Realization of the Hadamard multiplex advantage using a programmable optical mask in a dispersive flat-field near-infrared spectrometer," Appl. Spectrosc. **54**, 1751–1758 (2000).
4. S. P. Love, "Programmable matched filter and Hadamard transform hyperspectral imagers based on micro-mirror arrays," Proc. SPIE **7210**, 721007 (2011).
5. S. T. McCain, M. E. Gehm, Y. Wang, N. P. Pitsianis, and D. J. Brady, "Coded aperture Raman spectroscopy for quantitative measurements of ethanol in a tissue phantom," Appl. Spectrosc. **60**, 663–671 (2006).
6. M. E. Gehm, S. T. McCain, N. P. Pltsianis, D. J. Brady, and P. Potuluri, "Static two-dimensional aperture coding for multimodal, multiplex spectroscopy," Appl. Opt. **45**, 2965–3183 (2006).
7. A. A. Wagadarikar, M. E. Gehm, and D. J. Brady, "Performance comparison of aperture codes for multimodal, multiplex spectroscopy," Appl. Opt. **46**, 4932–4942 (2007).
8. G. Nitzsche and R. Riesenberg, "Noise, fluctuation and HADAMARD-transform-spectrometry," Proc. SPIE **5111**, 273–282 (2003).
9. M. B. Chi, Y. H. Wu, D. D. Ge, W. C. Zhou, P. Hao, and Y. S. Liu, "Encoded error calibration for a coded aperture spectrometer based on deconvolution," Appl. Opt. **55**, 1500–1506 (2016).
10. M. B. Chi, P. Hao, Y. H. Wu, Y. S. Liu, and P. Zhang, "Avoiding the side-effect of high-performance spectrometers with coded apertures," Appl. Opt. **52**, 6467–6473 (2013).
11. G. Westheimer, "Spatial and spatial-frequency analysis in visual optics," Ophthalmic Physiol. Opt. **32**, 271–281 (2012).
12. A. Mrozack, D. L. Marks, and D. J. Brady, "Coded aperture spectroscopy with regularization via convex optimization," in *Signal Recovery and Synthesis* (Optical Society of America, 2011).
13. H. Arguello and G. R. Arce, "Coded aperture optimization for spectrally agile compressive imaging," J. Opt. Soc. Am. A **28**, 2400–2413 (2011).